Inorganic Chemistry

Article

pubs.acs.org/IC

Preparation of Copper Nitride (Cu_3N) Nanoparticles in Long-Chain Alcohols at 130−200 °C and Nitridation Mechanism

Takashi Nakamura,* Hiromichi Hayashi, Taka-aki Hanaoka, and Takeo Ebina

Research Center for Compact Chemical System, National Institute of Advanced Industrial Science and Technology (AIST), Nigatake 4-2-1, Miyagino-ku, Sendai, Miyagi, 983-8551, Japan

Supporting Information

ABSTRACT: In our laboratory, we are studying copper nitride (Cu_3N) nanoparticles as a novel conductive ink that is stable to oxidation and can be metallized at low temperature. In this study, Cu_3N nanoparticles prepared via the reaction of copper(II) acetate monohydrate with ammonia gas in long-chain alcohol solvents were characterized by X-ray diffraction analysis, transmission electron microscopy, Fourier transform infrared spectroscopy, and elemental analysis. In addition, we used thermogravimetry−differential thermal analysis to compare the thermal decomposition properties of the prepared Cu_3N particles and commercially available Cu_3N particles. The decomposition temperature of the prepared particles was more than 170 °C lower than that of the commercial particles. We also examined the influences of the reaction temperature and the alkyl chain length of the alcohol solvent on the product distribution of the reaction and the morphology of the particles. Our results indicated that increasing the solvent hydrophobicity and eliminating water from the reaction system by increasing the temperature affected the product distribution. On the basis of an observation of chromatic change of the reaction solvent and an analysis of the byproducts in the alcohol solvent after the reaction, we propose a mechanism for the formation of Cu_3N.

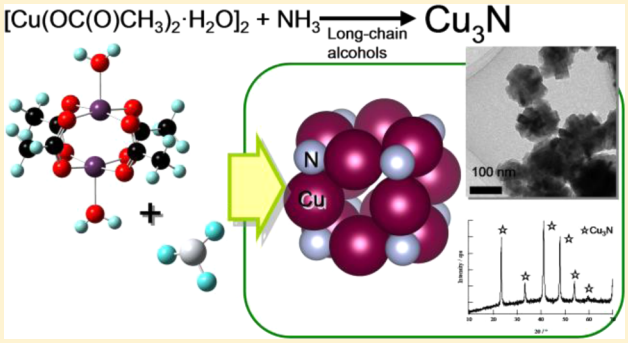

INTRODUCTION

Metal nitrides have unique catalytic, optic, and magnetic properties that are not shared by metal oxides. These properties arise from the localization of electrons on the anion lattices of metal nitrides. One of the most well-known metal nitrides in the semiconductor field is gallium nitride,[1] which is used to produce blue light-emitting diodes (LEDs) and blue lasers. Iron nitride, which is ferromagnetic, has also attracted considerable attention as an alternative to rare metals in the production of, for example, neodymium magnets.[2]

Copper nitride (Cu_3N), which has a cubic anti-ReO_3 crystal structure,[3] has been investigated as a material for resistive random access memory chips,[4] an optical recording medium,[5] an oxidation-resistant coating for copper, a catalyst for oxygen reduction,[6] and a conductive ink.[7] We believe that Cu_3N might be an optimal material for printed electronic devices.

Because of the relatively low cost and ionic migration resistance of copper nanoparticles, they are being actively explored as alternatives to silver nanoparticles as materials for printed electronic device interconnects.[8] However, because metallic copper is chemically unstable, copper nanoparticles are easily oxidized by water vapor or oxygen.[9] Obtaining the conductivity desired for the use of copper nanoparticles for interconnection commonly requires heat treatment at over 300 °C under a reducing gas atmosphere or vacuum conditions to metallize the material.[10,11]

To solve these problems associated with copper nanoparticles, we have been studying Cu_3N because it decomposes into copper and nitrogen at temperatures below 350 °C in the bulk state.[12] In addition, the fact that Cu_3N has been used as a coating for copper confirms that it is stable to oxidation. Furthermore, because Cu_3N nanoparticles exhibit a combination of desirable size-dependent characteristics (e.g., low decomposition temperature and melting point),[13−15] they are also considered to be excellent candidates as materials for electric wires in printed electronic devices.

Various investigators have reported the preparation of Cu_3N nanoparticles at high pressure or high temperature. For example, Choi and Gillan[16] heated copper chloride and sodium azide in toluene or tetrahydrofuran at 200 °C under solvothermal conditions (2.8−5.5 MPa), and Wang and Li[17] and Wu and Chen[6] heated copper nitrate in octadecylamine at ∼250 °C at atmospheric pressure. If Cu_3N could be prepared without the need for high pressure or temperature, Cu_3N nanoparticles could be easily mass produced.

In this paper, we report a novel method for preparing Cu_3N without high pressure or high temperature. Specifically, we prepared Cu_3N nanoparticles by heating copper(II) acetate monohydrate with ammonia gas in the presence of long-chain

Received: May 9, 2013
Published: December 26, 2013

alcohols. We characterized the crystal structure and morphology of the resulting particles, and determined the chemical state of the particle surfaces, as well as the decomposition temperature. We also examined the effects of the solvent on the product distribution of the reaction and on the morphology of the obtained particles. On the basis of our results, we propose a mechanism for the formation of Cu_3N under the tested reaction conditions.

EXPERIMENTAL SECTION

Materials. Copper(II) acetate monohydrate (Guaranteed Reagent grade) was purchased from Kanto Chemical Co. 1-Nonanol (>97%) was purchased from Tokyo Chemical Industry Co., and 1-octanol (>98%) was purchased from Wako Pure Chemical Industries. 1-Heptanol (>98%), 1-hexanol (>99%), and 1-pentanol (>98%) were purchased from Kishida Chemical Co. Ammonia gas (>99.999%) was purchased from Taiyo Nippon Sanso Co. All these reagents were used as supplied without further purification.

Typical Preparation Method for Cu_3N in Long-Chain Alcohols. Copper(II) acetate monohydrate (0.5 mmol) was dispersed in 1-nonanol (50 mL). The liquid dispersion was bubbled with ammonia (100 mL/min) and heated at 190 °C in an oil bath for 1 h (ramp time, 30 min; hold time, 30 min). During the heating, the color of the liquid changed dramatically, from a clear, deep blue to opaque yellow at 170 °C and finally to brown at 185 °C. The opaque liquid was supercentrifuged (30 000*g* for 60 min) to afford a brown powder, which was washed three times with *n*-hexane (yield, 81%).

X-ray Diffraction Analysis. The crystal structure of the obtained powder was characterized by X-ray diffraction (XRD) analysis (M21X, MacScience) with Cu Kα radiation at 40 kV and 200 mA at $2\theta = 10°-70°$ (recording interval, 0.002°).

Transmission Electron Microscopy. The morphology of the obtained powder was examined by means of transmission electron microscopy (TEM). For the TEM images shown in Figure 2 (shown later in this work), a JEM-3000F microscope (JEOL) operated at 300 kV was used to observe the product obtained by reaction in 1-nonanol at 190 °C. The images were recorded with a 1024 × 1024 pixel CCD camera. Samples were prepared by evaporating a drop of a suspension of the product diluted in *n*-hexane on a carbon-coated copper grid. A TECNAI G20 microscope (FEI) operated at 200 kV was used to record the images presented later in this paper in Figure 7. The images were recorded with a 1024 × 1024 pixel CCD camera. Samples were prepared by evaporating a drop of suspension of the product in *n*-hexane on a carbon-coated copper grid.

Fourier Transform Infrared Spectroscopy. Fourier transform infrared (FT-IR) spectra were measured with a Spectrum 1000 instrument (Perkin–Elmer) equipped with a Universal ATR sampling accessory (Perkin–Elmer). Spectra were recorded at room temperature from 650 cm^{-1} to 4000 cm^{-1} with a spectral resolution of 2 cm^{-1}.

Elemental Analysis. Elemental analysis was carried out with an EA 1110 instrument (CE Instruments) for carbon, hydrogen, and nitrogen. Oxygen was measured using a Flash EA 1112 instrument (CE Instruments).

Thermogravimetry and Differential Thermal Analysis. Thermogravimetry–differential thermal analysis (TG-DTA) was carried out with a Thermo Plus EVO II instrument (Rigaku) from 30 °C to 400 °C at a heating rate of 5 °C/min under argon and air in an aluminum pan. Alumina powder was used as a reference.

Scanning Electron Microscopy. Scanning electron microscopy (SEM) was carried out with a Model S-4800 microscope (Hitachi) operated at an acceleration voltage of 2 kV, an emission current of 10 μA, and a working distance of 3 mm.

Ultraviolet–Visible Spectroscopy. Ultraviolet–visible (UV-vis) spectroscopy was carried out with a Model U-2910 system (Hitachi). Spectra were recorded at room temperature from 250–1100 nm with a scanning speed of 800 nm/min with a spectral resolution of 1.0 nm. A quartz spectrophotometer cuvette with an optical path length of 10 mm was used.

Gas Chromatograph–Mass Spectrometry. Gas chromatography–mass spectrometry (GC-MS) was carried out with a Model CP-3800 gas chromatograph (Varian) attached to a Model 1200L mass spectrometer (Varian). An HP-INNOWax capillary column (Agilent, Model 19091N-133, 30 m in length, 0.25 mm i.d., 0.5 μm film thickness) was used for the chromatography. The carrier gas was helium, and the column flow rate was 1.2 mL/min. The inlet temperature was set at 230 °C, and the column temperature program was as follows: hold at 80 °C for 2 min, ramp to 240 °C at 20 °C/min, and hold at 240 °C for 20 min. Solutions for direct injection were prepared as follows: 2 mL of reaction solution was diluted with 10 mL of *n*-hexane and then filtered through a polytetrafluoroethylene (PTFE) filter (pore size = 0.1 μm). For direct injection, 1 μL of the sample solution was injected (split ratio 1:20) by means of a Combi PAL GC auto sampler (CTC Analytics GmbH). Mass spectra were measured with an acquisition delay of 2.50 min by means of the electron impact technique. The obtained mass spectra were compared to spectra in the NIST database for identification of each chemical compound.

RESULTS AND DISCUSSION

Preparation and Characterization of Cu_3N Nanoparticles. The crystal structure of the powder obtained from the reaction of copper(II) acetate monohydrate and ammonia was determined by XRD analysis (Figure 1). Based on the

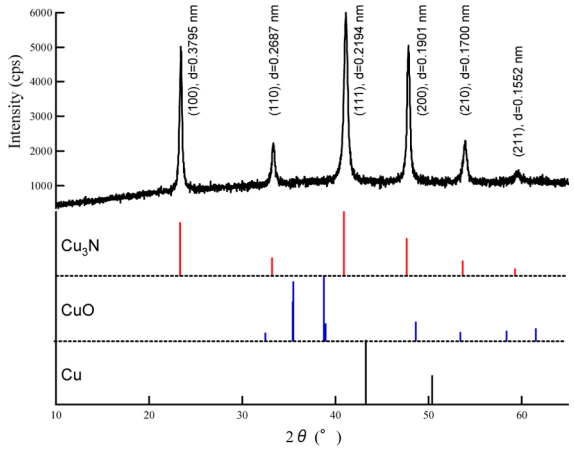

Figure 1. XRD pattern of prepared Cu_3N nanoparticles prepared in 1-nonanol heated at 190 °C for 1 h.

observed peaks at 23.40°, 33.34°, 41.12°, 47.84°, 53.92°, and 59.55°, which were attributed to (100), (110), (111), (200), (210), and (211) diffractions, respectively, the crystal structure was determined to be Cu_3N with an anti-ReO_3 structure (JCPDS File Card No. 47-1088). No peaks derived from Cu and CuO were observed. These results indicate that this method of synthesis produced single-phase Cu_3N.

The crystallite sizes of the obtained Cu_3N nanoparticles were determined by means of the Scherrer equation. We used the full width at half-maximum (fwhm) of the diffraction peaks and a value of 0.94 for the Scherrer constant. The crystallite sizes from the (100), (110), and (111) peaks were estimated to be 28.2, 26.0, and 20.2 nm, respectively.

We used TEM to observe the morphology and size of the Cu_3N particles (Figure 2). The Cu_3N particles had granular shapes and were <200 nm in diameter. They consisted of angular Cu_3N nanocrystals <20 nm on each side. The Cu_3N nanoparticles were homogenously prepared because these small particles were distributed in TEM observational under low magnification of view. From the diffraction pattern of the

dx.doi.org/10.1021/ic4011604 | *Inorg. Chem.* 2014, 53, 710–715

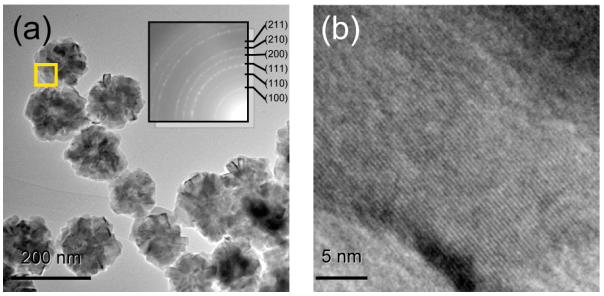

Figure 2. (a) TEM image of Cu_3N nanoparticles, along with diffraction pattern from the observed area (inset) and (b) magnified image of the yellow square in panel (a).

particles in observational area (Figure 2a), we confirmed that these particles had the crystal structure of Cu_3N.

We used the Fourier transform infrared (FT-IR) spectrum in the wavenumber range of 700−4000 cm^{-1} to determine the chemical-bonding state of the Cu_3N nanoparticles and of surfactants on the Cu_3N nanoparticles (Figure 3). To assign

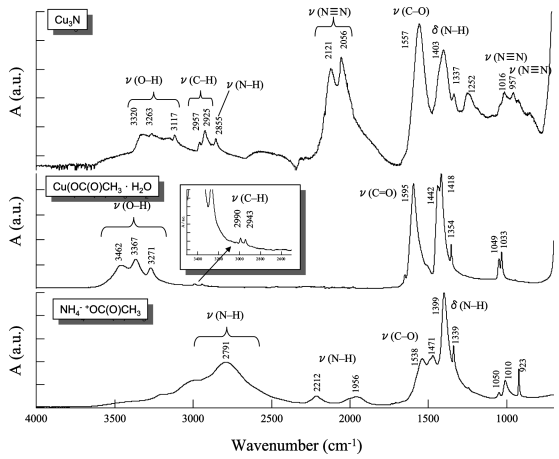

Figure 3. Fourier transform infrared (FT-IR) spectra of Cu_3N, copper(II) acetate monohydrate, and ammonium acetate.

peaks observed in the spectrum of the Cu_3N nanoparticles, we compared data for copper(II) acetate monohydrate, ammonium acetate, and various other compounds that had been previously reported.[18] Significant peaks with strong, sharp signals were observed at 2121, 2056, 1557, and 1403 cm^{-1}, and these peaks were attributed to ν(N≡N), ν(N≡N), ν(C−O), and δ(N−H), respectively. The spectrum indicated that not only carboxyl groups and ammonium ions but also N_2 was present on the surface of the Cu_3N nanoparticles. Free N_2 has a N≡N stretching peak at 2331 cm^{-1}; in contrast, because N_2 coordinated with a metal atom is a weak Lewis base, coordination shifts the stretching peak to 1850−2220 cm^{-1}. In the wavenumber range of 2850−3320 cm^{-1}, we observed peaks that we attributed to acetic acid, ammonium, and long-chain alcohol attached to the surface of the particles. Assigning all of the peaks to a specific compound was difficult because of peak broadening and overlap.

To estimate the organic compound content on the surface of Cu_3N nanoparticles, elemental analyses on nitrogen, carbon, hydrogen, and oxygen were carried out. The elemental contents (in wt %) were as follows: N, 6.5; C, 1.9; H, 0.3; and O, 6.0. By subtracting the measured contents from the total, the content of copper was estimated at 85.3 wt % in the sample. From these estimated values, the ratio by weight of Cu to N was estimated at 13.1 (Cu/N). The value of the ratio was in agreement with the calculated ratio of 13.6. Residual elemental contents (in wt %), except Cu and N, were recalculated as follows: C, 23.2; H, 3.6; and O, 73.2. If acetate ions are on the surface of Cu_3N nanoparticles, the content of oxygen is more than that of calculated value ($C_2H_3O_2$: C, 40.7; H, 5.1; O, 54.2 wt %). This error indicates that oxygen adsorbs on the surface of Cu_3N nanoparticles.

We compared the particle sizes and thermal decomposition properties of our prepared Cu_3N nanoparticles with those of commercially available Cu_3N (Santa Cruz Biotechnology). Scanning electron microscopy (SEM) indicated that the particle diameter of the prepared Cu_3N was 100−200 nm (Figure 4a), whereas that of the purchased Cu_3N was >1 μm

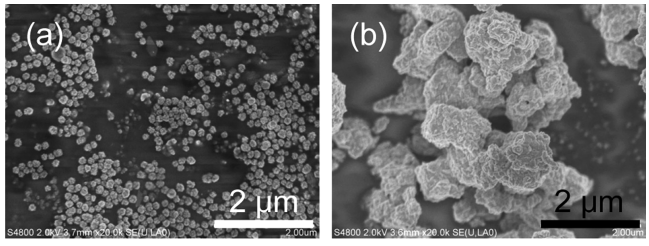

Figure 4. Scanning electron microscopy (SEM) images of (a) Cu_3N prepared in 1-nonanol at 190 °C and (b) purchased Cu_3N.

(Figure 4b). We used thermogravimetry−differential thermal analysis (TG-DTA) under argon to measure the decomposition temperatures of both of the Cu_3N samples (Figure 5). The

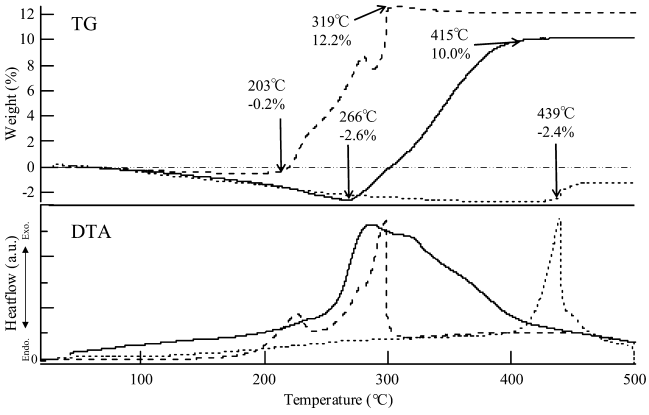

Figure 5. Thermogravimetry−differential thermal analysis (TG-DTA) curves of prepared Cu_3N powder under argon (solid line), prepared Cu_3N powder under the air (dashed line), and purchased Cu_3N powder under argon (dotted line).

prepared Cu_3N showed a loss in weight up to 266 °C. At higher temperatures, the weight of the sample increased, after an exothermic peak with a maximum at 287 °C. The purchased Cu_3N lost weight up to 439 °C, and at higher temperatures, the weight of the sample increased, and an exothermic peak with a maximum at 439 °C was observed. This comparison indicates that the decomposition temperature of the prepared Cu_3N was more than 170 °C lower than that of the purchased Cu_3N.

We also used XRD to characterize the crystal structure of the prepared Cu_3N powder after it had been heated at 500 °C under argon during TG-DTA (see Figure 1S in the Supporting

dx.doi.org/10.1021/ic4011604 | Inorg. Chem. 2014, 53, 710−715

Information). The diffraction pattern of the heated powder was that of CuO, and when the powder was heated under argon, no Cu diffraction pattern derived from the Cu_3N was observed. Unlike previous investigators, we were unable to trace the decomposition of Cu_3N to Cu and N_2.[3,5]

To consider desorption of nitrogen from Cu_3N nanoparticles, the TG-DTA curves of samples heated different atmospheres between argon and air in the TG-DTA furnace were compared. Calculated changes in the weight of decomposition (from Cu_3N to 3Cu) and oxidation (from Cu_3N to $(CuO)_3$) were −6.9% and 10.8%, respectively. The minimum of weight of the Cu_3N nanoparticles measured under argon was obtained −2.6% at 266 °C. The minimum of weight of the Cu_3N nanoparticles measured under air was obtained −0.2% at 203 °C. By using inert atmosphere by argon flow, the additional weight-loss of −2.4% was observed because of desorption of nitrogen from Cu_3N.

Influence of the Long-Chain Alcohol Solvent and the Reaction Temperature on the Product Distribution and the Morphology of the Prepared Particles. We also used XRD analysis to investigate how the length of the alkyl chain of the alcohol solvent affected the reaction of copper(II) acetate monohydrate with ammonia gas (Figure 6). Cu_3N nanoparticles were obtained when 1-nonanol, 1-octanol, or 1-heptanol was used as a solvent; both Cu_3N and CuO were obtained in 1-hexanol; and only CuO was obtained in 1-pentanol. We determined the morphology of the prepared particles by means of TEM (see Figures 2 and 7). The products of the reactions in 1-nonanol, 1-octanol, and 1-heptanol were granular particles with diameters of <300 nm. The reaction in 1-hexanol produced large particles that had diameters of several hundred nanometers and were covered with small particles 10−20 nm in diameter. The product obtained from 1-pentanol consisted of small particles with diameters of 10−20 nm. We determined that the 10−20 nm particles obtained from 1-hexanol and 1-pentanol were CuO on the basis of the corresponding peaks in the XRD patterns (Figure 6). Furthermore, from the fact of broad shape of the corresponding peaks, it is investigated that CuO are nanocrystallized. The crystallite size of CuO formed in 1-hexanol and 1-pentanol are estimated 9.7 and 6.5 nm, respectively, at $2\theta = 38.6°$ by means of the Scherrer equation.

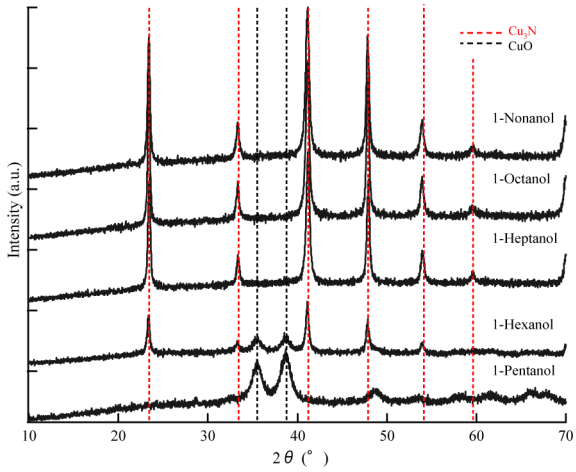

Figure 6. XRD patterns of Cu_3N powders prepared in various long-chain alcohols heated for 1 h. The reaction temperatures for 1-nonanol, 1-octanol, 1-heptanol, 1-hexanol, and 1-pentanol were 197, 174, 165, 150, and 130 °C, respectively.

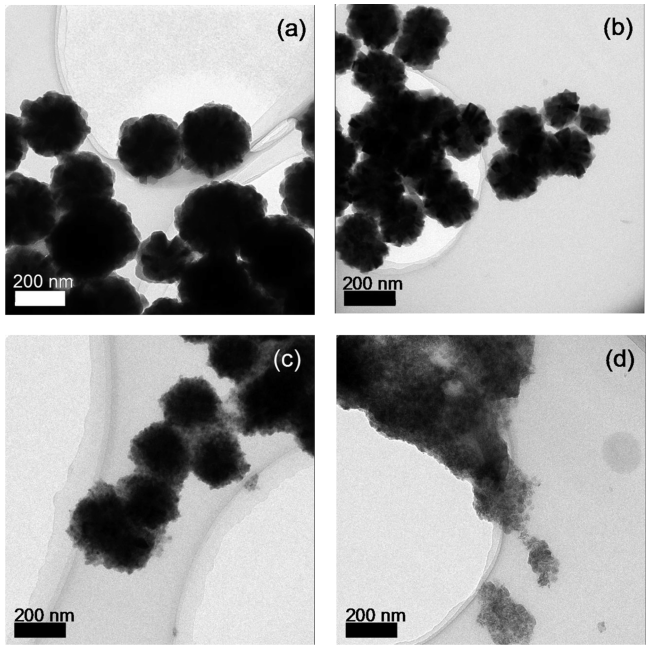

Figure 7. TEM images of Cu_3N particles prepared in (a) 1-octanol, (b) 1-heptanol, (c) 1-hexanol, and (d) 1-pentanol.

We initially speculated that the product differences observed for the various solvents were due to differences in reaction temperature. The results described above were for reactions carried out near the boiling point of the solvent (that is, at 10−20 °C below the boiling point). To evaluate this possibility, we investigated the products obtained from the various alcohol solvents at different reaction temperatures (Table 1). The reactions in 1-nonanol and 1-octanol afforded Cu_3N at all the tested reaction temperatures. In contrast, the reaction in 1-heptanol produced a single-phase of Cu_3N, a mixture of Cu_3N and CuO, or a single phase of CuO at 165, 150, or 130 °C, respectively. In 1-hexanol, the reaction produced a mixture of Cu_3N and CuO at 150 °C and a single phase of CuO at 130 °C. In 1-pentanol, the reaction produced a single phase of CuO at 130 °C.

Table 1. Products Obtained from Reactions of Copper(II) Acetate Monohydrate and Ammonia in Various Long-Chain Alcohols and at Various Temperatures

	Products Obtained			
solvent	130 °C	150 °C	near the solvent boiling point[a]	boiling point (°C)
1-nonanol	Cu_3N	Cu_3N	Cu_3N	214
1-octanol	Cu_3N	Cu_3N	Cu_3N	195
1-heptanol	CuO	Cu_3N, CuO	Cu_3N	176
1-hexanol	CuO	Cu_3N, CuO		158
1-pentanol	CuO			139

[a]The exact reaction temperatures for 1-nonanol, 1-octanol, and 1-heptanol were 197, 174, and 165 °C, respectively.

Based on these results, we concluded that increasing the solvent hydrophobicity by increasing the alkyl chain length and increasing the temperature in order to eliminate water from the

dx.doi.org/10.1021/ic4011604 | Inorg. Chem. 2014, 53, 710−715

reaction medium were essential. The small amount of water derived from the copper(II) acetate monohydrate and water formed by the esterification reaction between acetate anion and the long-chain alcohol (as described in the Discussion of the reaction mechanism below) dissolved in 1-heptanol, 1-hexanol, or 1-pentanol and then reacted with the Cu ion to form CuO.

Mechanism of the Nitridation Reaction. For the nitridation of copper or copper salts, several researchers have been reported previously. First, Juza and Hahn reported on issues concerning the synthesis and characterization of Cu_3N in 1938.[19] For the synthesis of Cu_3N particles, Zachwieja and Jacobs suggested a mechanism for ammonothermal synthesis for Cu_3N microsized crystals.[20] Choi and Gillan reported a mechanism for obtaining Cu_3N nanocrystals by a reaction copper chloride with sodium azido in toluene or tetrahydrofuran under solvothermal conditions.[16] Wang and Li reported a mechanism for obtaining Cu_3N nanocrystals by heating copper nitrate in octadecylamine.[17] Previously reported mechanisms in solution synthesis are suggested regarding vigorous conditions such as high pressures or high temperatures. In this study, we propose a mechanism for the nitridation of copper ion under a mild condition from a comprehensive result obtained by visible observation for color of solution, UV-vis spectroscopy, and analysis on residues in the solution after preparation of Cu_3N nanoparticles. Herein, we propose that under our reaction conditions, Cu_3N was produced by following reaction steps: (1) formation of copper(II) ammine complex, (2) reduction of Cu^{2+} to Cu^+ by the long-chain alcohol, and (3) successive reaction between Cu^+ and ammonia.

Formation of the Copper(II) Amine Complex. As the start of the reaction, the color of solution was change from green to blue by bubbling ammonia gas into 1-nonanol including copper(II) acetate monohydrate. To confirm the spectra of the solutions before and after ammonia bubbling, UV-vis absorption spectra were measured (see Figure 2S in the Supporting Information). Before bubbling ammonia gas, the spectrum showed a peak having a local maximum value at 700 nm attributed to $d-d$ transition of the Cu^{2+} ion.[21] After bubbling ammonia gas, the local maximum value at 700 nm shifts to a value at 635 nm. This value indicates the formation of the copper(II) ammine complex.[22]

Reduction of Copper Ion. Based, in part, on the fact that GC-MS analysis of the supernatant solution after the preparation of Cu_3N revealed the presence of nonyl acetate and 9-octadeceneamide (see Supporting Information), we propose the following reaction scheme.

Reduction of Cu^{2+} by 1-nonanol would afford Cu^+ and nonyl aldehyde. Under our reaction conditions, however, no nonyl aldehyde was observed, because it underwent Cu^+- or Cu^{2+}-catalyzed reaction with ammonia to form nonaneamide (see Scheme 1).[23] Moreover, in this reaction, the terminal of the alkyl chain of the nonaneamide reacted with the hydroxyl group of the 1-nonanol to form 9-octadeceneamide (see Scheme 2)

Scheme 1

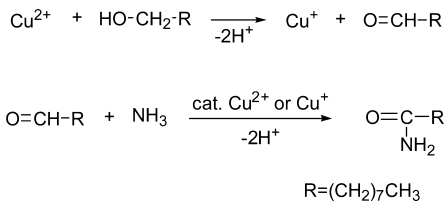

Scheme 2

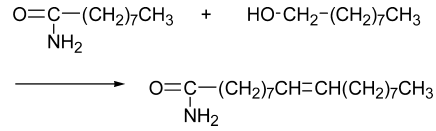

through a cross-coupling reaction. However, this mechanism of the cross-coupling reaction is still unclear. In addition, a chromatic change of reaction solution from blue to yellow suggested the formation of Cu^+ ions. The Cu^+ ion has no light absorption band in the visible region, because of $d10$ electron configuration. However, by formation of copper(I) complex, an light absorption band is made in the 350−500 nm region due to metal-to-ligand charge transfer (see Figure 6S in the Supporting Information).[24,25] By the light absorption in the region of violet, the color of solution was observed to be yellow, which is the complementary color of violet.

Nitridation of Copper Ion. Once Cu^{2+} is reduced, it must react with nitrogen if Cu_3N is to be formed. In this reaction, ammonia works as the nitrogen source. For the observation of the solution color under the reaction, the yellow color at 165 °C changed to opaque brown within 30 s. The fact means that the generation of Cu^+ immediately reacts with ammonia to form Cu_3N. (See Scheme 3.)

Scheme 3

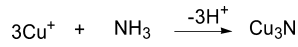

For the nitridation, it is crucial that ammonia remains in contact with Cu ions at the temperature at which reduction of Cu^{2+} is started. Although the ammonia coordinated on the Cu ion easily separates at high temperature, a continuous supply of ammonia must be available. When the ammonia gas was changed to nitrogen gas at 100 °C, copper nanoparticles were formed, because of the desorption of ammonia coordinated on the Cu ion at temperatures over 100 °C.

Esterification of Acetate Anion with Long-Chain Alcohol. As stated above, we also obtained an acetate ester (nonyl acetate) as a byproduct of the reaction. We believe that this byproduct was generated during the nitridation of Cu^+, via reaction of an acetate anion derived from copper(II) acetate monohydrate with 1-nonanol to form nonyl acetate and water.

Our proposed mechanism for the reaction of copper(II) acetate monohydrate and ammonia in long-chain alcohols differs from previously reported nitridation mechanisms. Because of the long-chain alcohol working as a reductant, ammonia as a nitrogen source easily reacts with the Cu ion to form Cu_3N under mild conditions, without high temperature and high pressure.

CONCLUSIONS

Cu_3N nanoparticles ~200 nm in diameter were prepared by the reaction of copper(II) acetate monohydrate with ammonia gas in long-chain alcohols. Comparison of the thermal decomposition properties of the prepared Cu_3N nanoparticles and purchased Cu_3N powder revealed that the decomposition temperature of the prepared nanoparticles was more than 170 °C lower than that of the purchased Cu_3N powder. The reaction was favored by increasing the hydrophobicity of the solvent (by increasing the alkyl chain length) and by eliminating water from the reaction system (by increasing the

dx.doi.org/10.1021/ic4011604 | Inorg. Chem. 2014, 53, 710−715

reaction temperature). By discussing a chromatic change of the solvent and analyzing ultraviolet−visible light (UV-vis) spectra and the byproducts of the reaction, we determined that the formation of Cu_3N likely occurred via the following three steps: (i) the formation of copper(II) ammine complex, (ii) reduction of Cu^{2+} to Cu^{+} by the long-chain alcohol, and (iii) subsequent quick reaction of Cu^{+} with ammonia.

■ ASSOCIATED CONTENT

Supporting Information

XRD pattern of the prepared particles after heating during TG-DTA, UV-vis absorption spectra of the 1-nonanol solution including copper(II) acetate monohydrate with and without ammonia bubbling, and GC-MS results. This material is available free of charge via the Internet at http://pubs.acs.org.

■ AUTHOR INFORMATION

Corresponding Author

*Fax: +81-22-237-3057. E-mail: nakamura-mw@aist.go.jp.

Funding

This work was financially supported by a grant from the A-STEP (Adaptable and Seamless Technology Transfer Program through Target-Driven R&D) program of the Japan Science and Technology Agency (Feasibility Study Stage, No. AS232Z00276C).

Notes

The authors declare no competing financial interest.

■ ACKNOWLEDGMENTS

We thank Misa Hayashida, Ph.D. (National Metrology Institute of Japan) for her assistance with the TEM observations.

■ REFERENCES

(1) Akasaki, I. *J. Cryst. Growth* **2007**, *300*, 2−10.
(2) Yamashita, S.; Masubuchi, Y.; Nakazawa, Y.; Okayama, T.; Tsuchiya, M.; Kikkawa, S. *J. Solid State Chem.* **2012**, *194*, 76−79.
(3) Paniconi, G.; Stoeva, Z.; Doberstein, H.; Smith, R. I.; Gallagher, B. L.; Gregory, D. H. *Solid State Sci.* **2007**, *9*, 907−913.
(4) Zhu, W.; Zhang, X.; Fu, X.; Zhou, Y.; Luo, S.; Wu, X. *Phys. Status Solidi A* **2012**, *209*, 1996−2001.
(5) Asano, M.; Umeda, K.; Tasaki, A. *Jpn. J. Appl. Phys., Part 1* **1990**, *29*, 1985−1986.
(6) Wu, H.; Chen, W. *J. Am. Chem. Soc.* **2011**, *133*, 15236−15239.
(7) Ji, A. L.; Lu, N. P.; Gao, L.; Zhang, W. B.; Liao, L. G.; Cao, Z. X. *J. Appl. Phys.* **2013**, *113*, 43705.
(8) Deng, D.; Cheng, Y.; Jin, Y.; Qi, T.; Xiao, F. *J. Mater. Chem.* **2012**, *22*, 23989−23995.
(9) Dement'eva, O. V.; Rudoy, V. M. *Colloid J.* **2012**, *74*, 668−674.
(10) Kim, Y.; Lee, B.; Yang, S.; Byun, I.; Jeong, I.; Cho, S. M. *Curr. Appl. Phys.* **2012**, *12*, 473−478.
(11) Jeong, S.; Woo, K.; Kim, D.; Lim, S.; Kim, J. S.; Shin, H.; Xia, Y.; Moon, J. *Adv. Funct. Mater.* **2008**, *18*, 679−686.
(12) Nosaka, T.; Yoshitake, M.; Okamoto, A.; Ogawa, S.; Nakayama, Y. *Appl. Surf. Sci.* **2001**, *169*, 358−361.
(13) Dick, K.; Dhanasekaran, T.; Zhang, Z. Y.; Meisel, D. *J. Am. Chem. Soc.* **2002**, *124*, 2312−2317.
(14) Castro, T.; Reifenberger, R.; Choi, E.; Andres, R. P. *Phys. Rev. B* **1990**, *42*, 8548−8556.
(15) Mudunkotuwa, I. A.; Rupasinghe, T.; Wu, C.-M.; Grassian, V. H. *Langmuir* **2012**, *28*, 396−403.
(16) Choi, J. L.; Gillan, E. G. *Inorg. Chem.* **2005**, *44*, 7385−7393.
(17) Wang, D.; Li, Y. *Chem. Commun.* **2011**, *47*, 3604−3606.
(18) Nakamoto, K. *Infrared and Raman Spectra of Inorganic and Coordination Compounds*; Wiley−Interscience: New York, 1997.
(19) Juza, R.; Hahn, H. *Z. Anorg. Allg. Chem.* **1938**, *239*, 282−287.
(20) Zachwieja, U.; Jacobs, H. *J. Less-Common Met.* **1990**, *161*, 175−184.
(21) Spessard, J. E. *Spectrochim. Acta A* **1970**, *26*, 297−306.
(22) Bjerrum, J.; Ballhausen, C. J.; Jørgensen, C. K. *Acta Chem. Scand.* **1954**, *8*, 1275−1289.
(23) Bantreil, X.; Fleith, C.; Martinez, J.; Lamaty, F. *ChemCatChem* **2012**, *4*, 1922−1925.
(24) Irving, H.; Williams, R. J. P. *J. Chem. Soc.* **1953**, 3192−3210.
(25) Blaskie, M. W.; McMillin, D. R. *Inorg. Chem.* **1980**, *19*, 3519−3522.